The Journal of Immunology

IFNAR1 Controls Progression to Cerebral Malaria in Children and CD8 $^{+}$ T Cell Brain Pathology in *Plasmodium berghei*–Infected Mice

Elizabeth Ann Ball, Maria Rosário Sambo, Madalena Martins, Maria Jesus Trovoada, Carla Benchimol, João Costa, Lígia Antunes Gonçalves, António Coutinho and Carlos Penha-Gonçalves

J Immunol 2013; 190:5118-5127; Prepublished online 12 April 2013;
doi: 10.4049/jimmunol.1300114
http://www.jimmunol.org/content/190/10/5118

The Journal of Immunology is published twice each month by
The American Association of Immunologists, Inc.,
9650 Rockville Pike, Bethesda, MD 20814-3994.

Print ISSN: 0022-1767 Online ISSN: 1550-6606.

IFNAR1 Controls Progression to Cerebral Malaria in Children and CD8$^+$ T Cell Brain Pathology in *Plasmodium berghei*–Infected Mice

Elizabeth Ann Ball,* Maria Rosário Sambo,*,†,‡ Madalena Martins,*,§ Maria Jesus Trovoada,*,¶ Carla Benchimol,‡ João Costa,* Lígia Antunes Gonçalves,* António Coutinho,* and Carlos Penha-Gonçalves*

Development of cerebral malaria (CM), a severe and fatal form of clinical *Plasmodium falciparum* infection, results from a damaging cascade of vascular, inflammatory, and immunological host responses that leads to brain injury. Progression to CM can be modified by host genetic factors. Our case-control study in Angolan children aimed at highlighting the role of IFN (α, β) receptor 1 (*IFNAR1*) in progression to CM. We report a robust association between *IFNAR1* and CM protection, as well as detailed studies showing analogous protection from experimental CM in *Ifnar1*$^{-/-}$ mice infected with *P. berghei* ANKA. We developed a novel cell-transfer protocol that enables spleen cell priming in the absence of disease. This led to the discovery that IFNAR1 expression in CD8$^+$ T cells is crucial and can abrogate resistance to experimental CM in *Ifnar1*$^{-/-}$ mice. Splenic CD8$^+$ T cells from *Ifnar1*$^{-/-}$ mice are functionally activated upon infection, yet are unable to mediate experimental CM development within the brain tissue. Our findings prove that IFNAR1 signaling unleashes CD8$^+$ T cell effector capacity, which is vital for CM, and raises the hypothesis that the cohesive role of *IFNAR1* in both human and mouse CM operates through CD8$^+$ T cell triggering. ***The Journal of Immunology*****, 2013, 190: 5118–5127.**

Cerebral malaria (CM) is a severe, and often fatal, complicated form of *Plasmodium falciparum* malaria, affecting mostly children in endemic regions (1–3). Although adhesion and sequestration of infected RBCs (iRBCs) in brain microvasculature leads to blood vessel occlusion and is central to CM pathogenesis (4), immunological mechanisms operating during the development of CM remain unclear.

Accessibility to human tissues limits research into understanding the progression and control of CM development in humans (5). Therefore, use of the mouse model, termed "experimental CM" (ECM), has enabled researchers to uncover cellular and molecular components occurring in CM. Recent articles addressed the relevance of the mouse model of ECM and emphasized the need for identifying consistent factors between the mouse model and human studies (6–9). Because such factors are seldom confirmed, confounding lists of players in CM development have emerged. However, one factor remaining implicit are CD8$^+$ T cells (10, 11), although the exact mechanisms that drive their pathogenesis in CM remain unclear. Additionally, the role of cytokines in human CM development was brought to light in recent genetic studies (reviewed in Ref. 12). Initial studies by Hill and coworkers (13, 14) began exploring the necessary role of type I IFN (type I IFN) in CM progression and found that genetic variants in *IFNAR1* led to protection from CM development. Because IFNAR1 is the key signaling receptor mediating type I IFN activity (15) and is expressed on virtually every cell surface (16, 17), the impact that type I IFN has on the immune response is vast. In particular, type I IFN was shown to be involved in the priming of CD8$^+$ T cells (18, 19) and in the generation of a robust immune response to infection (20, 21). Recent studies addressed the actions of type I IFN, through the IFNAR1 receptor, in response to hemozoin derivatives (22), as well as in controlling parasite burden upon *Plasmodium* infection (23). However, the exact caliber of *IFNAR1* action in CM development remains unexplored.

We performed a genetic study to analyze *IFNAR1* involvement in the progression of CM versus uncomplicated malaria (UM). We selected children, the primary risk group of severe malaria, from an area of Angola where malaria transmission is perennial (24). We report in this article that variants of *IFNAR1* strongly associate with CM protection, which drove the use of *Ifnar1*$^{-/-}$ mice to interrogate the action of *IFNAR1* in CM pathogenesis. We describe ECM protection in *Ifnar1*$^{-/-}$ mice and, through design of a novel cell-transfer protocol, we expose the necessity of IFNAR1 expression in CD8$^+$ T cells during the development of ECM.

Materials and Methods

Patient and control samples

A total of 272 children, living in Luanda and ranging from 6 mo to 13 y of age, were enrolled in the current study. Ethical permission for this study was granted by the Ethical Committee of the Hospital Pediátrico David Bernardino in Luanda, appointed by the Angolan Ministry of Health. Written, informed consent was obtained from the parents or guardians of each child. Subjects were selected from patients at Hospital Pediátrico David Bernardino. The details of the data set were described previously

*Instituto Gulbenkian de Ciência, 2781-156 Oeiras, Portugal; †Faculdade de Medicina, Universidade Agostinho Neto, Luanda, Angola; ‡Hospital Pediátrico David Bernardino, Luanda, Angola; §Neurological Clinical Research Unit, Institute of Molecular Medicine, Faculty of Medicine, University of Lisbon, 1649-028 Lisboa, Portugal; and ¶Centro National de Endemias, São Tomé, Saõ Tome e Príncipe

Received for publication January 18, 2013. Accepted for publication March 6, 2013.

This work was supported by Fundação para a Ciência e a Tecnologia fellowship grants: SFRH/BD/33564/2008 (to E.A.B.) and SFRH/BPD/29354/2006 (to M.M.).

Address correspondence and reprint requests to Dr. Carlos Penha Gonçalves, Instituto Gulbenkian de Ciência, Rua da Quinta Grande, 6, 2780-156 Oeiras, Portugal. E-mail address: cpenha@igc.gulbenkian.pt

The online version of this article contains supplemental material.

Abbreviations used in this article: BBB, blood–brain barrier; CM, cerebral malaria; ECM, experimental cerebral malaria; GrB, granzyme B; hap, haplotype; iRBC, infected RBC; *PbA*, *Plasmodium berghei* ANKA-GFP; PI, postinfection; RT, room temperature; SNP, single nucleotide polymorphism; UM, uncomplicated malaria.

www.jimmunol.org/cgi/doi/10.4049/jimmunol.1300114

(25). Briefly, samples were collected from children aged 6–156 mo, between February 2005 and May 2007, and included 130 patients with CM and 142 patients with UM. Malaria was diagnosed on the basis of a positive asexual parasitemia detected on a Giemsa-stained thick smear (26). CM was defined according to the World Health Organization criteria: a coma score < 3 on the Blantyre Scale for children <60 mo or a coma score < 7 on the Glasgow Scale for children ≥ 60 mo. Meningitis and encephalitis were ruled out by cerebrospinal fluid analysis after lumbar puncture. Exclusion criteria were different known etiologies of encephalopathy and hypoglycemia (glycemia < 40 mg/dl). Patients with consciousness disturbances or with other diseases were also excluded from this group. The UM group represents patients with malaria diagnosis and febrile illness without any clinical finding suggestive of other causes of infection and with no manifestations of severe malaria.

Genotyping

Genomic DNA was extracted from whole blood using the Chemagen Magnetic Bead technology. DNA preparations were quantified using PicoGreen reagents, according to the supplier's instructions. Twenty-seven single nucleotide polymorphisms (SNPs) covering the *IFNAR1* region were initially genotyped using the Sequenom's iPlex assay (San Diego, CA) and the Sequenom MassArray K2 platform by the Genomics Unit of the Instituto Gulbenkian de Ciência.

Extensive quality control was performed using eight HapMap (http://hapmap.ncbi.nlm.nih.gov/) controls of diverse ethnicity, Hardy–Weinberg equilibrium with $p > 0.01$, and a minimum 90% call rate for each SNP. Genotype determinations were performed blinded to affection status. Only SNPs with minor allele frequency $> 1\%$ in both groups were analyzed for association. Nine SNPs in *IFNAR1* (rs224359, rs2252930, rs12626750, rs2834197, rs2226300, rs2254315, rs1012943, 2843996, and 2254305) did not meet the quality control criteria and were excluded. Samples with $<75\%$ call rate and duplicates were excluded from analysis; a total of 33 samples was excluded. The final data set used in the analysis consisted of 239 children: 110 CM patients (mean age, 54.6 mo) and 129 UM patients (mean age, 49.1 mo).

Association testing

The $\chi 2$ tests for Hardy–Weinberg equilibrium in both groups, allelic and haplotypic association of SNPs with progression to CM, and linkage disequilibrium plots were performed using Haploview 4.2 (27). A diagram with representation of the allelic genetic-association results was produced by the snp.plotter R package (28). Association analyses were performed with logistic regression and adjusted for potential confounding effects of age using the SNPassoc v.1.4-9 package (29) implemented in R freeware (http://cran.r-project.org/). Results were considered suggestive below the conventional probability level of 0.05. Bonferroni corrections for multiple tests were carried out to exclude type I errors (the significance level for 18 tests is set at p value $< 2.78\ E-3$).

Animals

Male, 8–12-wk-old C57BL/6, B6.Ly5.1, *Ifnar1*$^{-/-}$, and BALB/c mice were bred and used as provided by the Instituto Gulbenkian de Ciência in-house animal facility. *Ifnar1*$^{-/-}$ mice (*Ifnar1*$^{\text{-tm-Agt}}$) (30) were originally a gift to the institute from Michel Aquet, Institute of Molecular Biology, University of Zurich, Switzerland. *Ifnar1*$^{-/-}$ mice were backcrossed onto the C57BL/6 background (98.7–99.36% C57BL/6 background outside of the congenic region, as confirmed by the animal facility at Instituto Gulbenkian de Ciência). All procedures were in accordance with national regulations on animal experimentation and welfare, as approved by the Instituto Gulbenkian de Ciência Ethics Committee.

Parasite, infection, and ECM disease assessment

All infections used 1×10^6 *Plasmodium berghei ANKA*-GFP (*PbA*)-parasitized iRBCs (31) given via i.p injection. Frozen iRBC stocks were expanded in C57BL/6 mice prior to infection. Parasitemia was determined as the percentage of GFP$^+$ RBCs, using flow cytometry analysis (FACScan Cell Analyzer; Becton Dickinson) and noninfected RBCs as negative control. ECM development was monitored from day 5 postinfection (PI), including head deviations, paralysis, ataxia, and convulsions (32). ECM-susceptible mice developed symptoms at days 6–7 PI and died within 4–5 h. Mice resistant to ECM died around days 22–25 from anemia and hyperparasitemia without displaying neurologic symptoms.

Blood–brain barrier integrity

Upon display of ECM-induced coma in C57BL/6 mice, the experimental groups of mice were injected with 100 μl 2% Evan's blue dye (Sigma), sacrificed 1 h postinjection, and perfused intracardially with 15 ml ice-cold PBS. Brains were dissected, weighed, and immersed in 2 ml formamide (Merck), covered at 37°C for 48 h, to allow extraction of Evan's blue dye; images were taken after the 48 h period. Noninfected mice from each group were used as controls. Absorbance of dye was measured at 620 and 740 nm using spectrophotometry (Thermo Spectronic Helios Delta). Using a standard curve, data were calculated and expressed as μg Evans blue dye/mg brain tissue.

Histology

Infected C57BL/6 and *Ifnar1*$^{-/-}$ mice were sacrificed upon observation of clinical signs of ECM in C57BL/6 mice, ~day 6 PI. Noninfected C57BL/6 and *Ifnar1*$^{-/-}$ mice were used as controls and sacrificed at the same time point. For H&E staining, brains were carefully removed, fixed in 10% neutral-buffered formalin, embedded, sectioned (4 μm), mounted with Entellan (Merck, Darmstadt, Germany), and stained with H&E, following standard procedures. CM and brain pathology were assessed by routine histopathology in coronal brain sections of the same anatomical location. Bright-field images were captured using a Leica DMD108 microscope (Leica Microsystems); 10× (numerical aperture: 0.40) and 40× (numerical aperture: 0.95) objectives were used. Adobe Photoshop software (Adobe) was used to compose images and adjust the contrast.

Gene expression

Infected C57BL/6 and *Ifnar1*$^{-/-}$ mice were sacrificed at days 5–7 PI. *Ifnar1*$^{-/-}$ mice were also sacrificed at days 9 and 11 PI; C57BL/6 mice were not collected at these time points due to death from ECM. Noninfected C57BL/6 and *Ifnar1*$^{-/-}$ mice were used as controls and represent day 0. Brains were dissected, fast frozen in liquid nitrogen, and stored at −80°C. Brains were then homogenized, and a final brain weight of 20 mg was used for total RNA extraction (RNeasy Mini Kit; QIAGEN). RNA quality was determined using Nanodrop, and a final elution of 50 μl was extracted. One microgram of total RNA was converted to cDNA (Transcriptor High Fidelity cDNA Synthesis Kit; Roche) using random hexamer primers, and a final volume of 10 μl the cDNA reaction was diluted 1:3 in RNase-free water to be used for mRNA quantification. *Tnf-α* and *Il-10* mRNA was quantified using TaqMan Gene Expression Assays from ABI (Mm00443258_m1 and Mm99999062_m1, respectively). *P. berghei ANKA* rRNA was quantified using specific primer sequences: forward 5′-CCG ATA ACG AAC GAG ATC TTA ACC T-3′, reverse 5′-CGT CAA AAC CAA TCT CCC AAT AAA GG-3′ and probe 5′-ACT CGC CGC TAA TTA G-3′ (FAM/MGB), all with TaqMan Universal PCR Master Mix. T lymphocyte (*Cd3e*) expression was quantified using a specific primer sequence, forward 5′-TCT CGG AAG TCG AGG ACA GT-3′ and reverse 5′-ATC AGC AAG CCC AGA GTG AT-3′ (33), using Power SYBR Green PCR Master Mix (Applied Biosystems). Gene expression–quantification reactions were performed on an ABI Prism 7900HT system, according to the manufacturer's instructions; a total volume of 10 μl PCR reactions was amplified for 45 cycles. Relative quantification of specific mRNA was normalized to the mouse housekeeping gene *ACTB* (Mouse ACTB Endogenous Controls; ABI), used in multiplex PCR with the target genes and calculated using the ΔΔCt method.

Presensitization protocol

For infected blood donor mice, blood was collected by mandibular vein puncture into an Eppendorf tube containing 10 μl heparin (Heparina Leo; LEO Pharmaceutical Products) from infected mouse at day 6 PI, upon display of ECM symptoms and when parasitemia was ~30%. Parasitemia was measured to calculate injection of 4×10^6 iRBCs into cell donor mice. Collected blood was then placed on ice in a 50-ml Falcon tube and irradiated at 20,000 rad (Gammacell 2000; Mølsgaard Medical). Irradiated iRBCs were then resuspended in PBS and injected i.p. into cell donor mice. At day 6 postirradiated iRBC injection, cell donor mice were sacrificed, and purified spleen cell populations were injected into recipient mice; recipient mice were left noninfected or were infected with 1×10^6 *PbA* i.p. 1 h after transfer. Parasitemia and ECM development were monitored from day 5 PI. For control noninfected blood donor mice, mice were bled, and an equivalent volume of noninfected RBCs was irradiated and diluted in PBS in the same manner as above.

Spleen cell transfers

Single-cell suspensions were prepared from spleens of cell donor mice. For total spleen cell transfers, cells were washed twice in PBS, counted in a hemocytometer, resuspended in PBS, and injected at 5×10^6/100 μl into recipient mice. For spleen CD8$^+$ cell transfers, cells were washed twice in PBS, 2% FCS and incubated with anti-mouse CD8–Alexa Fluor 647 Ab (clone YTS169; in-house production) for 30 min on ice. For CD8$^+$Ly5.1/2$^+$ cell transfers, cells were incubated with anti-mouse CD8–Alexa Fluor 647 Ab (clone YTS169; in-house production), anti-mouse CD45.1-FITC Ab

(clone 820; BD Pharmingen), or anti-mouse CD45.2-PE Ab (clone 104.2; in-house production) for 30 min on ice. Stained cells were washed in PBS, 2% FCS and sorted (FACSAria Multicolor Cell Sorter; Becton Dickinson) by combining lymphocyte morphological gating and relevant Ab labels. For $CD8^+$ transfers, cells were collected as purified $CD8^+$ cells and $CD8^-$ (depleted) groups of cells. For $CD8^+Ly5.1/2$ transfers, cells were gated for $CD8^+$ cells, within which $CD45.1^+$ or $CD45.2^+$ populations were collected. Purified cell populations were washed in PBS and counted. Cells were injected i.v. at 3×10^6/100 μl into recipient mice. Respective groups of recipient mice were then infected with 1×10^6 iRBCs/100 μl *PbA* 1 h after cell transfer. Mice were monitored for parasitemia and ECM development from day 5 PI.

Analysis of spleen cells

Single-cell suspensions were prepared from spleens of infected C57BL/6 and *Ifnar1*$^{-/-}$ mice at day 5 PI; noninfected mice from both groups were used as control. Cells used for total cell counts and activation profile were prepared as single-cell suspensions: from 5 ml total cells, 200 μl/sample was plated in a 96-well round-bottom plate, and cells were centrifuged; pelleted; resuspended in Fc Block for 20 min on ice; washed in PBS, 2% FCS; and resuspended in either anti-mouse CD8–Alexa Fluor 647 Ab (clone YTS169; in-house Ab) or CD4–Alexa Fluor 647 (clone GK 1.5; in-house Ab) with CD44-FITC (clone IM7; BD Pharmingen 553133) and CD62L-PE (clone Mel 14; eBioscience 12-0621-85) for 20 min on ice. Cells were then washed, resuspended in 100 μl PBS, 2% FCS plus 20 μl propidium iodide (1 μg/ml; P-4170; Sigma) and 10 μl 5×10^5 beads (Beckman Coulter nominal 10 μm Latex Beads). For intracellular staining, cells were washed and resuspended in RBC lysis buffer; washed and resuspended in 100 μl RPMI 1640 medium supplemented with 10% FCS, 10 U/ml Pen-Strep, 1% sodium pyruvate, 1% HEPES 1 M, 1% L-glutamine, and 0.01% 2-ME; centrifuged; and resuspended in 200 μl RPMI 1640 supplemented medium containing 10 μg/ml brefeldin A for fixation of intracellular cytokine production and 100 ng/ml of PMA and 500 ng/ml ionomycin used for cell stimulation. Cells were stimulated at 37°C, 5% CO_2 for 4 h. Cells were then processed for extracellular staining; cells were centrifuged, pelleted, resuspended in Fc Block for 20 min on ice, washed in PBS, 2% FCS, and resuspended in anti-mouse CD8–Alexa Fluor 647 Ab (clone YTS169; in-house Ab) for 20 min on ice. Cells were then washed and resuspended in 2% paraformaldehyde for fixation for 30 min at room temperature (RT), washed twice in PBS, resuspended in 200 μl PBS, 2% FCS, and stored at 4°C overnight. The following day, cells were pelleted and resuspended in permeabilization buffer (10% saponin in PBS, 2% FCS) for 10 min at RT in preparation for intracellular staining. Cells were then washed, pelleted, and incubated with anti-mouse granzyme B (GrB)–FITC (clone NGZB; eBioscience) and anti-mouse IFN-γ–PE (clone XMG1.2; BD Pharmingen) for 30 min at RT. Cells were then washed twice in permeabilization buffer and then twice in PBS, 2% FCS and resuspended in 150 μl PBS, 2% FCS plus 5×10^5 beads (as before). All cell analyses were performed using a FACSCalibur cell analyzer and FlowJo software (version 7). Single-staining preparations were used for control compensation of double-staining analysis.

Analysis of brain-sequestered leukocytes

Infected C57BL/6 and *Ifnar1*$^{-/-}$ mice were sacrificed at day 6 PI and perfused pericardially (as described above), and brains were placed in 10 ml HBSS supplemented with Collagenase VIII (0.2 mg/ml; Sigma). Brains were then smashed and incubated for 30 min at 37°C. Each sample was passed through a 100-μm strainer and centrifuged for 10 min at 1500 rpm. Supernatant was discarded, and samples were resuspended in 10 ml PBS and centrifuged. Samples were resuspended in 10 ml 30% Percoll gradient (Percoll; GE Healthcare, BioSciences) and centrifuged for 20 min at 2500 rpm at RT, without brake. The supernatant was aspirated carefully, and the pellet was resuspended in 50 ml PBS and centrifuged. The supernatant was discarded, and each sample pellet was resuspended to a final volume of 200 μl. Cells were centrifuged and resuspended in 100 μl RBC lysis buffer, incubated for 5 min at RT, washed twice in 200 μl PBS, 2% FCS, resuspended in supplemented RPMI 1640 medium, and prepared for extra- and intracellular staining and analysis, as described above.

Statistical analysis

The nonparametric Mann–Whitney *U* test was used for analysis when comparing data from two groups of mice. One-way ANOVA was used to compare three or more groups of data. Survival analysis was assessed by

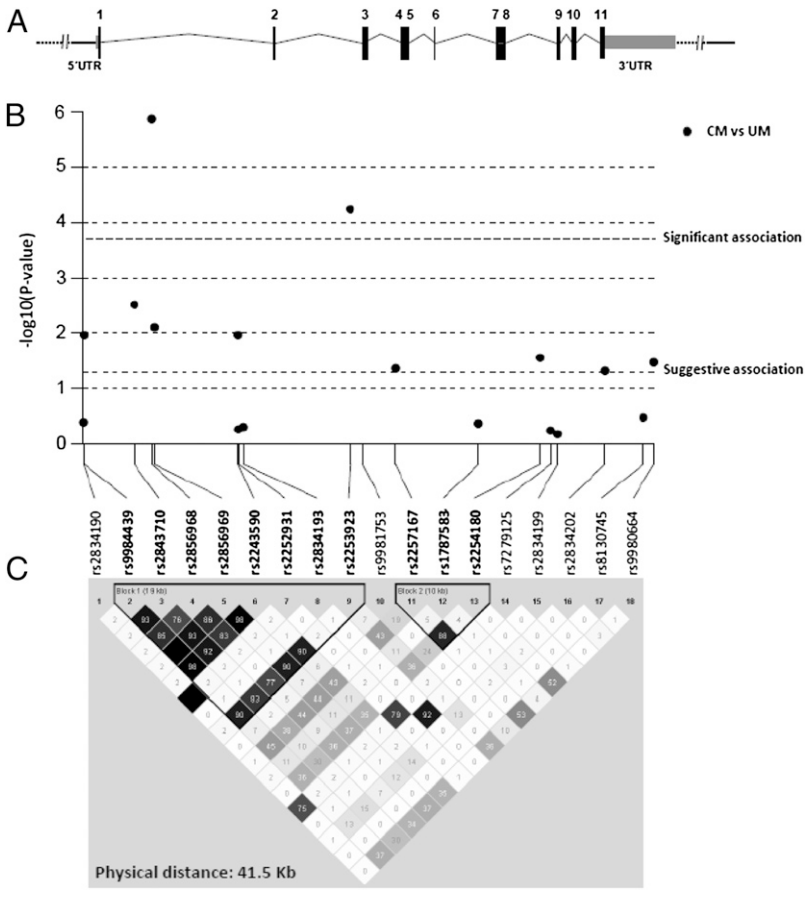

FIGURE 1. *IFNAR1* gene variants protect against malaria progression to CM syndrome. Results of genotypic association tests under the dominant model at 18 *IFNAR1* SNPs, depicted at the bottom of the horizontal axis according to relative physical distance. (**A**) Scaled diagram of the *IFNAR1* gene structure: exons are marked with their corresponding number, 5′ untranslated region and 3′ untranslated region are represented by gray boxes, and introns are represented by black lines between exons. (**B**) Genotypic *p* values of association tests were obtained by comparing 110 cases of CM with 129 patients with UM using logistic regression and adjusted for age. Thresholds for suggestive association ($p = 0.05$) and for significant association after multiple testing Bonferroni correction ($p = 2.78\ E{-}3$) are represented. (**C**) Linkage disequilibrium plot representing pairwise R^2 in a gray scale and revealing the two hap blocks in the analyzed region. This diagram is an adaptation of the figure produced by the snp.plotter R package and the linkage disequilibrium map obtained from Haploview 4.2.

the log-rank test. All tests were performed using Prism GraphPad 4. The p values ≤ 0.05 were considered statistically significant.

Results

IFNAR1 variants are associated with protection against clinical progression to CM

The *IFNAR1* gene has been associated with severe forms of malaria (13, 14). In this study, we used a cohort of Angolan children to identify *IFNAR1* genetic variants that specifically modify the risk for progressing from uncomplicated forms of malaria to CM syndrome. We compared genotype frequencies of SNPs in infected children that developed CM ($n = 110$) versus children that presented with clinically UM ($n = 129$). After age correction, 8 of 18 *IFNAR1* SNPs showed a suggestive association ($p < 0.05$) with progression to CM (Fig. 1B), possibly under a dominant mode of action (Supplemental Table II). The two markers having the strongest association with progression to CM, rs2856968 ($p = 1.33E{-}6$) and rs2253923 ($p = 5.77E{-}5$), remained significantly associated after conservative Bonferroni correction for multiple testing ($p < 2.78E{-}3$) (Fig. 1B). Because the two SNPs are in strong linkage disequilibrium ($r^2 = +0.77$), this result suggests a single genetic effect in CM protection (Fig. 1D).

Haplotypic-association analysis of eight SNPs in the 5′ region of *IFNAR1* (encompassing upstream regulatory region intron 1 and intron 2) identified one haplotype (hap) that shows robust association with CM protection ($P_{hap} = 6.89E{-}7$; $OR_{hap} = 0.34$). Conversely, the most frequent haplotype for the same eight SNPs shows an increased risk for CM progression ($P_{hap} = 8.0E{-}4$; $OR_{hap} = 1.87$). Together, this genetic evidence strongly suggests that specific minor frequency alleles of the *IFNAR1* gene provide protection against CM. This suggests a decisive role for *IFNAR1* during the inflammatory response to malaria infection and, specifically, at dictating progression to CM.

Ifnar1$^{-/-}$ *mice are protected from development of ECM and brain pathology*

We used the mouse model of ECM to ascertain whether *IFNAR1* is involved in inflammation evoked by malaria infection (6). In line with a recent report (22), we observed that *PbA* infection in *Ifnar1*$^{-/-}$ mice led to strong resistance to ECM (75% ECM resistance, Fig. 2A) compared with susceptible C57BL/6 control mice. *Ifnar1*$^{-/-}$ mice that resist ECM development die between days 25 and 30 from anemia and hyperparasitemia and showed parasitemia comparable to C57BL/6 mice up to day 6 PI (Fig. 2B). This indicated that ECM resistance in *Ifnar1*$^{-/-}$ mice was not related to decreased peripheral parasite burden.

Disruption of the blood–brain barrier (BBB) is a hallmark of ECM pathology (34). We analyzed infected and noninfected C57BL/6, *Ifnar1*$^{-/-}$, and ECM-resistant BALB/c mice for barrier compromise using Evans blue. Like BALB/c mice, *Ifnar1*$^{-/-}$ mice displayed no BBB compromise (Fig. 3A, 3B), as opposed to C57BL/6 mice, which showed abundant dye leakage in the brain. Histopathological analysis of infected C57BL/6 brain sections exhibited prominent mononuclear cell accumulations within brain microvessels (Fig. 3D), evidence of disruption of vessel walls and endothelial cell destruction (Fig. 3E), and parenchymal hemorrhagic lesions containing iRBCs (Fig. 3F). In contrast, ECM-resistant *Ifnar1*$^{-/-}$ mice displayed mild intravascular accumulation of mononuclear cells (Fig. 3H), intact endothelial cells (Fig. 3I), and absence of hemorrhagic lesions with iRBCs seen within the lumen of blood vessels only (Fig. 3J). These results show that, despite abnormal mononuclear accumulation within brain microvessels and the presence of intraluminal iRBCs, infected *Ifnar1*$^{-/-}$ mice do not exhibit pathology typical of ECM.

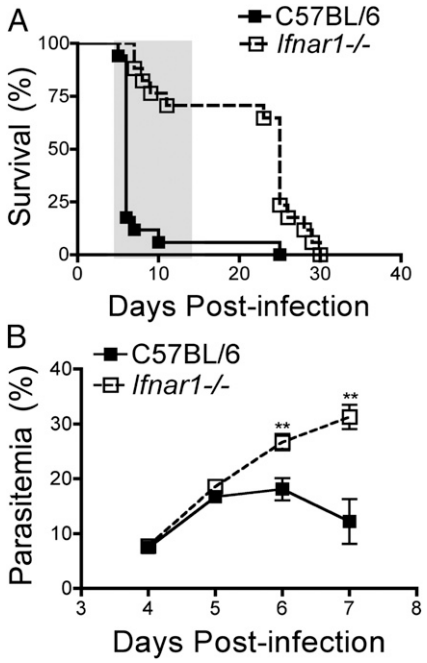

FIGURE 2. *Ifnar1*$^{-/-}$ mice are protected from ECM and show no decrease in parasite burden. C57BL/6 and *Ifnar1*$^{-/-}$ mice were infected with 1×10^6 *PbA*-infected RBCs via i.p. injection. (**A**) Survival curve ($n = 17$), log-rank test. Time window of C57BL/6 ECM development is shaded. (**B**) Parasitemia progression ($n = 17$). Data were collected from at least four independent experiments. $^{**}p = 0.0016$ (day 6 PI), $^{**}p = 0.0021$ (day 7 PI), unpaired, two-tailed t test.

Ifnar1$^{-/-}$ *mice display a delayed brain inflammatory response upon infection*

To further investigate the mechanisms underlying ECM protection in *Ifnar1*$^{-/-}$ mice, we evaluated cytokine production and parasite burden within the brain tissue of infected C57BL/6 and *Ifnar1*$^{-/-}$ mice. Comparison of *P. berghei* rRNA quantification showed no significant differences during the early time course of infection, strongly suggesting that ECM protection in *Ifnar1*$^{-/-}$ mice was not attributable to reduced brain parasite burden (Fig. 4A). We also observed that kinetics of *Cd3* mRNA expression in the brain leading up to ECM manifestations were slightly lower in *Ifnar1*$^{-/-}$ mice but not significantly different from C57BL/6 mice; this suggests that T cell migration to the brain during infection was not impaired in *Ifnar1*$^{-/-}$ mice (Fig. 4B). Nevertheless, we found that, in the brain of *Ifnar1*$^{-/-}$ mice, the expression of inflammatory markers (i.e., *Tnf* and *Il10*) had lower induction in the period preceding ECM onset and showed delayed kinetics compared with infected C57BL/6 mice. Overall, these results indicate that, despite the accumulation of iRBCs and the presence of T cells, *Ifnar1*$^{-/-}$ mice show a diminished exacerbation in their inflammatory responses, deterring the development of brain pathology within the time frame of ECM development.

Presensitization for cell transfer

We questioned in which cell type IFNAR1 was fundamental to cause ECM development in mice. To this end, we developed a novel cell-transfer protocol to determine the ability of individual cell types to restore ECM susceptibility in *Ifnar1*$^{-/-}$ mice (Fig. 5A). Donor mice were exposed to irradiated iRBCs, allowing relevant blood-stage parasite Ags to prime in vivo immune system cells that were then used in transfer experiments. The irradiated parasite is unable to reinvade RBCs; therefore, (exposed) donor mice do not develop parasitemia or ECM. We analyzed the T cell profiles

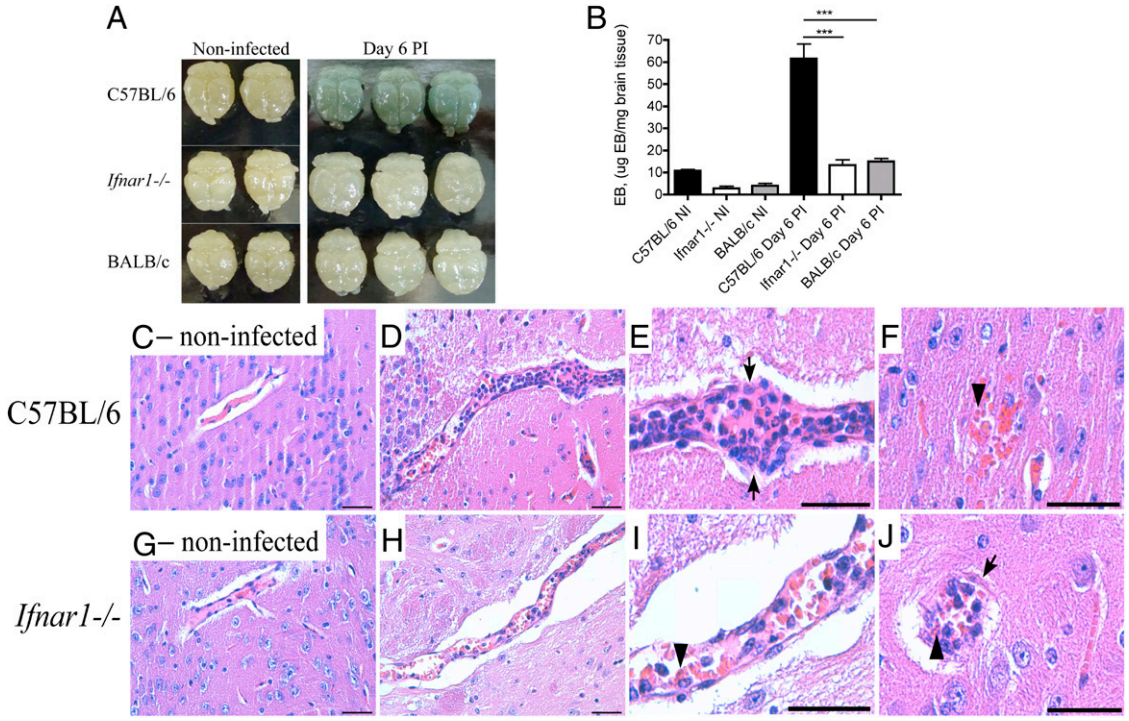

FIGURE 3. *Ifnar1*$^{-/-}$ mice are protected from BBB compromise and show reduced mononuclear cell accumulation in brain microvasculature. C57BL/6, *Ifnar1*$^{-/-}$, and BALB/c mice were infected with 1×10^6 *PbA* iRBCs i.p. and analyzed at day 6 PI. (**A**) BBB integrity was assessed in all infected groups of mice by Evan's Blue perfusion. Noninfected mice from each group were used as controls (n = 3–5 mice/group). Images are representative of two independent experiments. (**B**) Quantification of Evan's Blue dye was measured as micrograms of dye per milligram of brain tissue (n = 3–4 mice/group). ***$p \leq 0.001$, ANOVA, Tukey multiple-comparison test. Data are representative of two independent experiments. (**C**–**J**) H&E staining of brain sections from C57BL/6 and *Ifnar1*$^{-/-}$ mice (noninfected mice were used as controls). Mice were sacrificed upon display of ECM in C57BL/6 mice. Coronal sections of brain microvasculature and mononuclear cell accumulation in noninfected C57BL/6 mice (C), infected C57BL/6 mice (D–F), noninfected *Ifnar1*$^{-/-}$ mice (G), and infected *Ifnar1*$^{-/-}$ mice (H–J). Original magnification in (C), (D), (G), and (H) ×400 and in (F) and (J) ×1000; scale bars, 30 μm. Detail images of coronal sections of infected C57BL/6 mice showing absence of endothelial cells (E, arrows) and presence of hemorrhagic foci with iRBCs (F, arrowhead). Sections of infected *Ifnar1*$^{-/-}$ mice showing intact endothelial cells (J, arrow) and intraluminal iRBCs (I, J, arrowhead). Images are representative of three mice examined per group.

of C57BL/6 mice that received iRBCs, as well as mice that received irradiated iRBCs (Fig. 5B, 5C). We found that the numbers of CD8$^+$ T cells in mice that received irradiated iRBCs were not as high as those found in infected C57BL/6 mice but were similar in number to activated CD8$^+$ T cells (CD44^{hi} and CD62L^{low}) (Fig. 5B). We noted that CD4$^+$ T cell numbers and activation profile were not significantly different between mice that received irradiated iRBCs or iRBCs (Fig. 5C). Together, this suggests that irradiated iRBCs induce activation of both CD8$^+$ and CD4$^+$ T cells. A group of C57BL/6 cell donor mice was injected with irradiated iRBCs and then infected with 1×10^6 nonirradiated *PbA* iRBCs 7 d later (as per normal infection); all mice developed ECM and died by day 7 PI (data not shown). We concluded that our protocol does not confer protective immunity but rather is a protocol of immune cell presensitization that occurs in the absence of parasite expansion or disease development. We anticipate that this method will be useful in investigating pathogenic mechanisms of malaria blood-stage infection in future mouse models.

C57BL/6 spleen cells confer ECM susceptibility to Ifnar1$^{-/-}$ *mice*

Total splenocytes were transferred from C57BL/6 mice that had received irradiated iRBCs (cell donors) to *Ifnar1*$^{-/-}$ mice. Upon infection, recipient *Ifnar1*$^{-/-}$ mice showed 75% development of ECM, 6–12 d PI, within the ECM time frame of susceptible C57BL/6 mice (Fig. 5D). This demonstrates that C57BL/6 splenocytes presensitized to irradiated iRBCs are effective at restoring ECM susceptibility in *Ifnar1*$^{-/-}$ mice. In a control experiment, total splenocytes were transferred from C57BL/6 donor mice that had received noninfected irradiated RBCs to *Ifnar1*$^{-/-}$ mice. When infected 1 h posttransfer, recipient mice developed

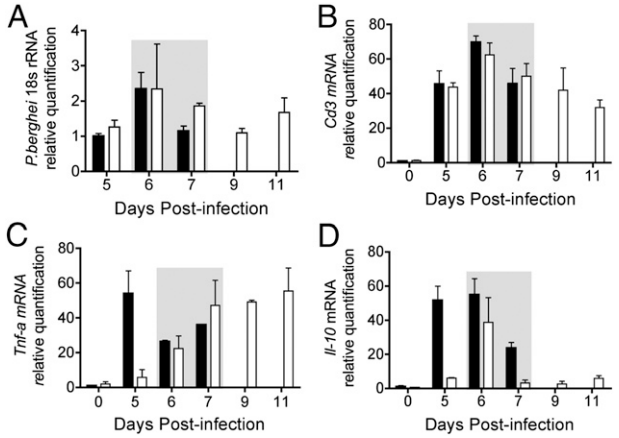

FIGURE 4. Parasite accumulation and brain-inflammation markers in infected *Ifnar1*$^{-/-}$ mice. C57BL/6 (black bars) and *Ifnar1*$^{-/-}$ (white bars) mice were infected with 1×10^6 *PbA* iRBCs i.p., and brain RNA was extracted at the indicated time points for RT-PCR quantification. (**A**) *P. berghei* rRNA relative quantification; day 5–infected C57BL/6 mice were used as a calibrator. Expression of *Cd3* (**B**), *Tnf-α* (**C**) and *Il-10* (**D**); noninfected C57BL/6 mice were used as a calibrator, represented as day 0 (n = 3–4 mice/group/d). Data are mean ± SD from one of two independent experiments. Time window of C57BL/6 ECM onset is shaded. Nonparametric Mann–Whitney U test.

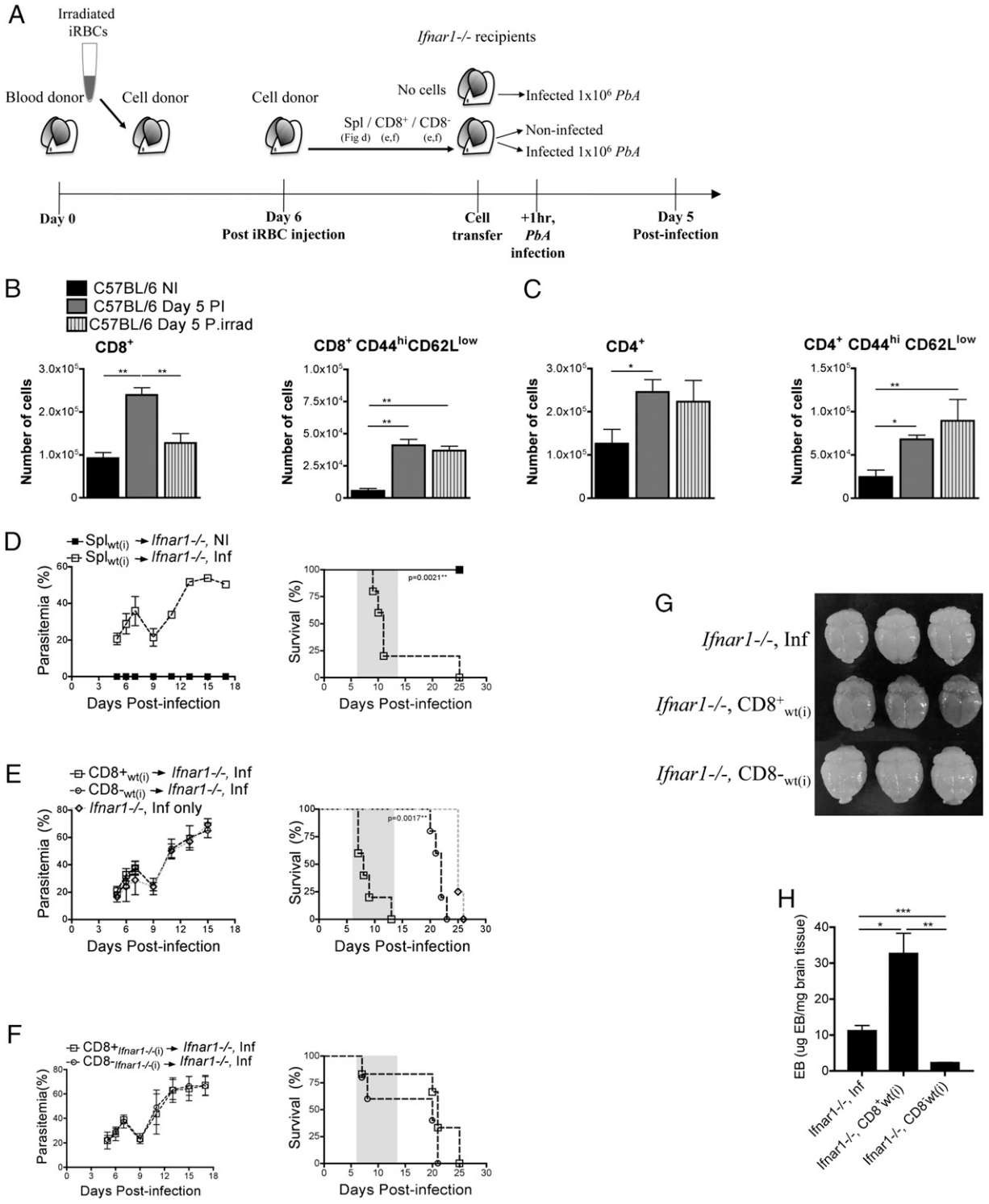

FIGURE 5. *Ifnar1*$^{-/-}$ mice succumb to ECM upon cell transfer of parasite-sensitized splenocytes, explicitly CD8$^+$ cells. (**A**) Schematic representation of presensitization protocol described in *Materials and Methods*. Total number and activation profile of splenic CD8$^+$ (**B**) and CD4$^+$ (**C**) T cells from C57BL/6 mice at 5 d postchallenge: noninfected (NI; black bar), infected with 1×10^6 *PbA* i.p. (gray bar), or injected with 4×10^6 irradiated iRBCs i.p. (striped bar) (n = 4–6 mice/group). *$p \leq 0.05$, **$p \leq 0.01$, nonparametric Mann–Whitney U test. (**D**) Parasitemia (*left panel*) and survival (*right panel*) curves of *Ifnar1*$^{-/-}$ mice that received total spleen cells from C57BL/6 pre-exposed donor mice; recipients were infected after transfer (□) or left noninfected (■). Parasitemia (*left panels*) and survival (*right panels*) curves of *Ifnar1*$^{-/-}$ mice that received sorted presensitized CD8$^+$ spleen cells (□) or sorted presensitized CD8$^-$ depleted spleen cells (○) from C57BL/6 pre-exposed cell donor mice (**E**) or *Ifnar1*$^{-/-}$ pre-exposed cell donor mice (**F**). Transfer control represents infected *Ifnar1*$^{-/-}$ mice that received no cells (◇) (n = 4–6 mice/group). Parasitemia: unpaired t test. Survival: log-rank test significant p values, ■ versus □ (in [D]) and □ versus ○ (in [E]). All significant differences are displayed. Each plot represents one of at least two independent experiments. Time window of ECM is shaded in survival plots. (**G**) Measurement of BBB compromise by Evans Blue perfusion in recipient *Ifnar1*$^{-/-}$ mice, as in (E) (n = 3–4 mice/group). (**H**) Quantification of Evans Blue (EB) dye (n = 3–4 mice/group). Data in (G) and (H) represent one of two independent experiments. *$p \leq 0.05$, **$p \leq 0.01$, ***$p \leq 0.001$, ANOVA, Tukey multiple-comparison test.

parasitemia like *Ifnar1*$^{-/-}$ mice that received infection only (no cell transfer). Neither group of mice developed ECM, with all mice dying around day 25 PI from anemia and hyperparasitemia (Supplemental Fig. 1). This shows that C57BL/6 splenocytes exposed to noninfected irradiated RBCs are unable to induce ECM susceptibility in *Ifnar1*$^{-/-}$ mice, indicating that RBC irradiation per se has no impact on ECM development in recipient mice. We then determined whether CD8$^+$ spleen cells induced ECM in *Ifnar1*$^{-/-}$ mice. Sorted CD8$^+$ or CD8$^-$ depleted cells, isolated from donor C57BL/6 mice that received irradiated iRBCs, were transferred into *Ifnar1*$^{-/-}$ mice (Fig. 5E). Recipient mice were then infected 1 h after cell transfer. Parasitemia did not differ between the two groups of mice compared with *Ifnar1*$^{-/-}$ mice that received infection only (and no cell transfer). In contrast, we found ECM development only in the group of *Ifnar1*$^{-/-}$ mice that received purified CD8$^+$ cells. This result indicates that transfer of presensitized C57BL/6 CD8$^+$ cells is sufficient to restore susceptibility to ECM in *Ifnar1*$^{-/-}$ mice. Upon transfer of presensitized *Ifnar1*$^{-/-}$ CD8$^+$ T cells to *Ifnar1*$^{-/-}$ mice, we found that recipient mice did not develop ECM; this led us to conclude that only CD8$^+$ IFNAR1$^+$ cells from exposed C57BL/6 mice were able to cause ECM (Fig. 5F). By assessing BBB integrity, we confirmed the ability of presensitized CD8$^+$ cells isolated from C57BL/6 mice to induce bone fide ECM. We observed BBB compromise only in *Ifnar1*$^{-/-}$ mice that received C57BL/6 CD8$^+$ cells and not in CD8$^-$ cell–depleted recipient mice (Fig. 5G, 5H). Together, these results show that IFNAR1 is critical for CD8$^+$ cell–mediated abrogation of ECM resistance in *Ifnar1*$^{-/-}$ mice.

Intrinsic CD8$^+$ T cell properties trigger ECM development

We modified our cell-transfer protocol to ascertain whether ECM induction was dependent on IFNAR1 expression in CD8$^+$ cells (Fig. 6A). CD8$^+$ cells were sorted from noninfected *Ifnar1*$^{-/-}$.Ly5.2 mice and transferred to previously nonlethally irradiated C57BL/6.Ly5.1 mice, allowing for the discrimination of endogenous and transferred CD8$^+$ populations. Ly5.1/5.2 chimeric mice then received irradiated iRBCs from a B6.Ly5.1 mouse. Seven days later, Ly5.1 CD8$^+$ and Ly5.2 CD8$^+$ cell populations were sorted (Fig. 6B) and transferred to *Ifnar1*$^{-/-}$ recipient mice. No differences in parasitemia progression were observed in either group compared with *Ifnar1*$^{-/-}$ mice that received no cell transfer and infection only (Fig. 6C). We found that only recipient *Ifnar1*$^{-/-}$ mice that had received Ly5.1 IFNAR1$^+$ CD8$^+$ cells developed ECM, showing 100% disease incidence, whereas recipients of Ly5.2 IFNAR1$^-$ CD8$^+$ cells maintained ECM resistance comparable to *Ifnar1*$^{-/-}$ mice that received no cell transfer and infection only. This strongly suggests that deficiency in IFNAR1 signaling in CD8$^+$ cells impairs their ability to induce ECM in *Ifnar1*$^{-/-}$ mice during *PbA* infection.

Ifnar1$^{-/-}$ *mice display differing activation states in spleen and brain tissue compared with C57BL/6 mice*

To investigate CD8$^+$ T cell impairments in *Ifnar1*$^{-/-}$ mice during *PbA* infection, we analyzed the activation and expansion of CD8$^+$ T cells in the spleen at day 5 PI, prior to ECM onset. We found a significant difference between noninfected C57BL/6 and *Ifnar1*$^{-/-}$ mice that was attenuated upon infection. This indicates that infection-driven CD8$^+$ T cell expansion was not impaired in *Ifnar1*$^{-/-}$ mice (Fig. 7A). Similarly, splenic CD8$^+$ T cells from *Ifnar1*$^{-/-}$ mice do not show impairments in GrB or IFN-γ expression upon infection (Fig. 7B, 7C). We also note that CD4$^+$ T cell expansion and activation, as measured by IFN-γ, are not hindered in *Ifnar1*$^{-/-}$ mice upon infection compared with C57BL/6 mice (Supplemental Fig. 2).

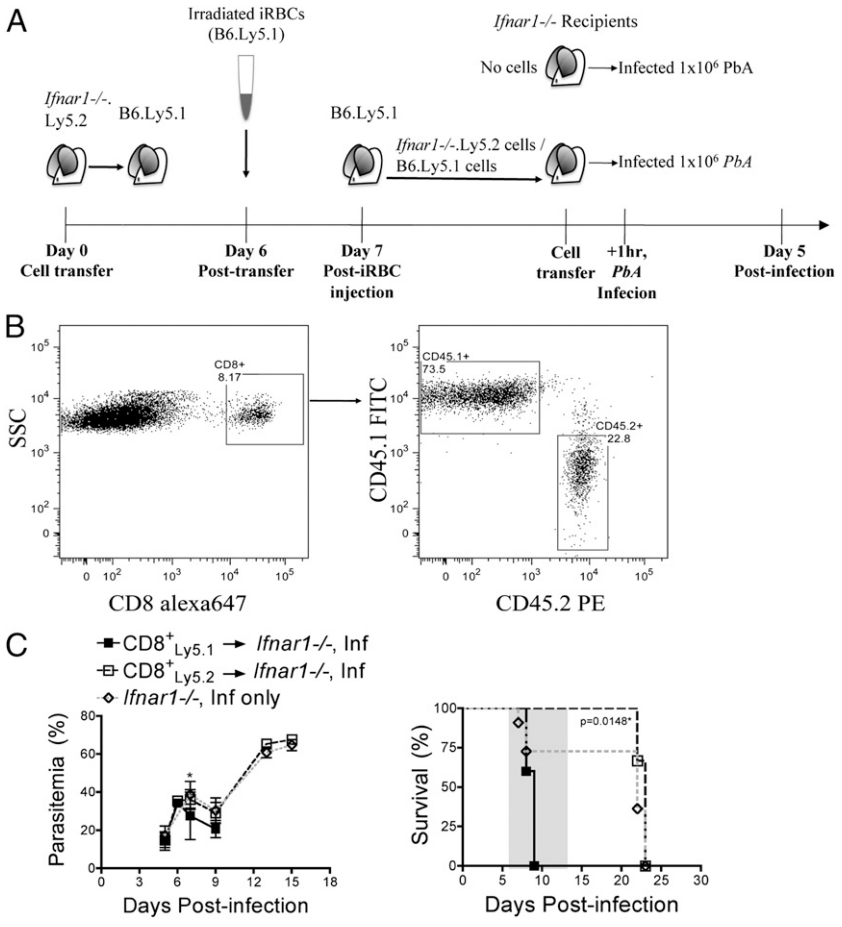

FIGURE 6. Intrinsic *Ifnar1*$^{-/-}$ CD8$^+$ cell impairment protects from ECM. (**A**) Schematic representation of experimental protocol. Noninfected *Ifnar1*$^{-/-}$ mice were used as donors of 5 × 10^6 CD8$^+$Ly5.2$^+$ spleen cells that were transferred to previously nonlethally irradiated B6.Ly5.1 recipient mice. Six days posttransfer, Ly5.1/Ly5.2 chimeric mice received 4 × 10^6 irradiated iRBCs from a previously infected B6.Ly5.1 mouse. (**B**) Seven days after iRBC infection, CD8$^+$Ly5.2$^+$ and CD8$^+$ Ly5.1$^+$ spleen cells were FACS sorted, as described in *Materials and Methods*. The sorted CD8$^+$ cell populations were injected back into *Ifnar1*$^{-/-}$ recipients, and mice were infected with 1 × 10^6 iRBCs 1 h after cell transfer. (**C**) Parasitemia (*left panel*) and survival (*right panel*) curves of *Ifnar1*$^{-/-}$ recipient mice that received either CD8$^+$Ly5.1$^+$ (■) or CD8$^+$Ly5.2$^+$ cells (□) from pre-exposed chimeras or no cell transfer and infection only as control (◇) (n = 3–12 mice/group). Data are pooled from three independent experiments. Time window of C57BL/6 ECM symptoms is shaded in survival plot. Parasitemia: unpaired t test between CD8$^+$Ly5.1$^+$ and CD8$^+$Ly5.2$^+$ recipient groups (*$p \leq 0.05$). Survival: *$p \leq 0.05$, log-rank test, ■ versus □.

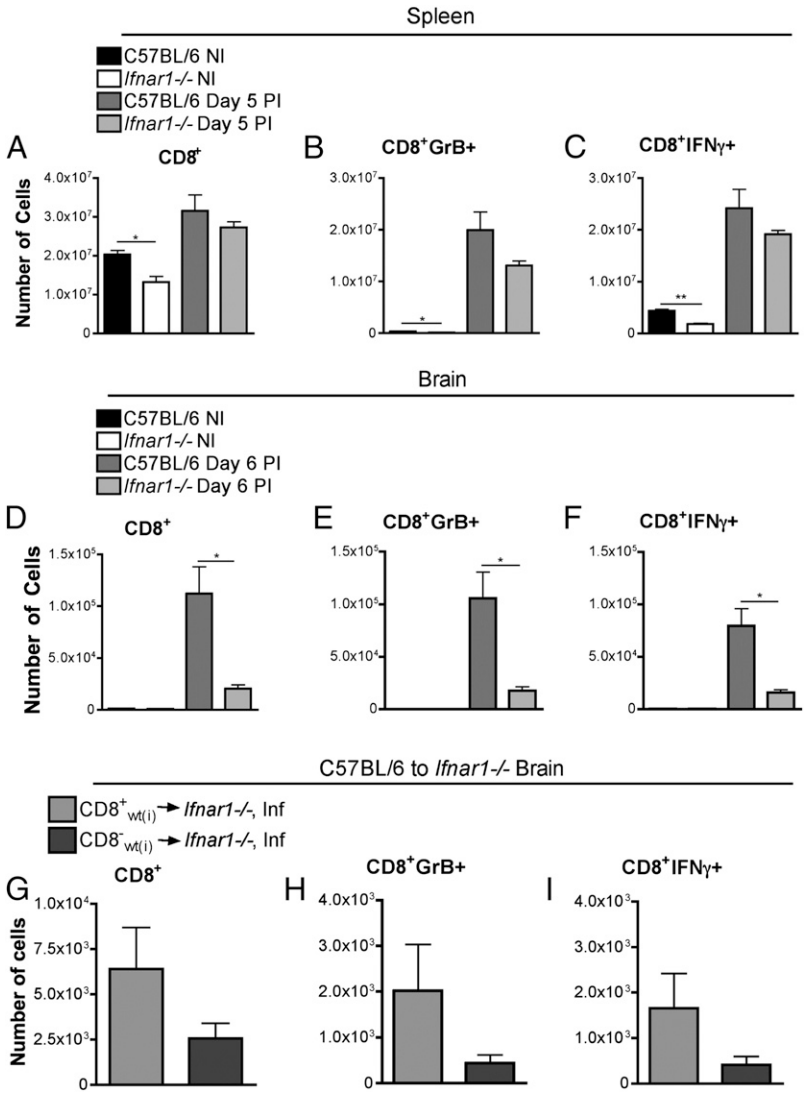

FIGURE 7. IFNAR1$^-$ CD8$^+$ T cells show activation upon infection but not accumulation in the brain. Numbers of CD8$^+$ T cells (**A**, **D**), GrB$^+$ CD8$^+$ T cells (**B**, **E**), and IFN-γ^+ CD8$^+$ T cells (**C**, **F**) of infected and noninfected C57BL/6 and *Ifnar1*$^{-/-}$ mice in the spleen (A–C) and perfused brains (D–F). Numbers of CD8$^+$ T cells (**G**), GrB$^+$ CD8$^+$ T cells (**H**), and IFN-γ^+ CD8$^+$ T cells (**I**) in perfused brains of *Ifnar1*$^{-/-}$ recipient mice that received sorted CD8$^+$ or CD8$^-$ depleted spleen cells from pre-exposed C57BL/6 donor mice. Mice were analyzed for CD8$^+$ T cells in the spleen on day 5 PI and in the brain on day 6 PI when C57BL/6 or *Ifnar1*$^{-/-}$ ECM-induced mice displayed symptoms of ECM development (n = 3–5 mice/group). Data are representative of three (A–F) or two (G–I) independent experiments. [(B), C57BL/6 noninfected group mean: 2.8×10^5; *Ifnar1*$^{-/-}$ noninfected group mean: 8.0×10^4]. $*p \leq 0.05$, $**p \leq 0.01$, nonparametric Mann–Whitney U test; all statistically significant differences are shown.

Likewise, we analyzed profiles of CD8$^+$ T cells from the brain of infected C57BL/6 and *Ifnar1*$^{-/-}$ mice at day 6 PI, upon display of end-stage ECM symptoms in control C57BL/6 mice. We found that the total number of CD8$^+$ T cells sequestered in the brain of *Ifnar1*$^{-/-}$ mice was significantly reduced compared with C57BL/6 mice (Fig. 7D). Nevertheless, the vast majority of brain-sequestered CD8$^+$ T cells in both *Ifnar1*$^{-/-}$ and C57BL/6 mice were activated and showed a cytotoxic profile (Fig. 7E, 7F). This indicates no faltering in sequestered *Ifnar1*$^{-/-}$ CD8$^+$ T cells to exhibit a cytotoxic profile, as supported by mean fluorescence intensity analysis of GrB and IFN-γ in CD8$^+$ T cells upon infection compared with C57BL/6 mice (Supplemental Fig. 3).

We confirmed these results by analyzing sequestered CD8$^+$ T cells on day 6 PI from *Ifnar1*$^{-/-}$ mice that received either CD8$^+$ T cells (and were restored with ECM susceptibility) or CD8$^-$ depleted cells. As expected, higher numbers of CD8$^+$ T cells, as well as GrB$^+$ and IFN-γ^+ CD8$^+$ T cells, were seen in the brain of mice that received CD8$^+$ T cell transfer (Fig. 7G–I). However, these results were not significantly different, suggesting that induction of ECM in *Ifnar1*$^{-/-}$ mice is not strictly dependent on accumulation of effector IFNAR1$^+$ CD8$^+$ T cells. Together, these results suggest that ECM resistance in *Ifnar1*$^{-/-}$ mice operates through impaired IFNAR1 signaling in CD8$^+$ T cells.

Discussion

This work strengthens the role of type I IFNs/IFNAR1 signaling in human cerebral malaria and uncovers the actions of IFNAR1 in ECM development. We found that *IFNAR1* genetic variants showed protection against progression to CM in a population of Angolan children. In Gambian children, two SNPs, which were identified in the *IFNAR1* gene in intron 3 and exon 4, were associated with severe malaria and CM (13). However, the study of Gambian, Kenyan, and Vietnamese populations (14) highlighted positive associations in the 5′ region of the *IFNAR1* locus. This was also found as a region of strong association in our study, suggesting that the 5′ region of the *IFNAR1* gene known to control transcriptional activity (35) represents a malaria-susceptibility factor throughout diverse populations. Furthermore, the design established in our study proved to be advantageous, allowing us to evaluate specifically the association of *IFNAR1* with disease progression from UM to CM. *IFNAR1* has also been associated with AIDS progression (15) and clinical presentation of hepatitis B virus infection (36), which allows the inference that *IFNAR1* variants can affect type I IFN responses and govern the course and progression of infectious diseases.

These results motivated the use of *Ifnar1*$^{-/-}$ mice to address the mechanisms underlying the pathogenesis of CM in the ECM mouse model. We found that protection from ECM in *Ifnar1*$^{-/-}$

mice was not controlled via a reduction in parasite burden. Conflicting results have been found; one study (22) showed no decrease in parasitemia when using *PbA* infection in *Ifnar1*$^{-/-}$ mice, whereas another study (23) reported a decrease in parasite burden upon *PbA*-GFP + luciferase infection. It remains to be determined whether different strains of *PbA* parasite dictate parasitemia burden in *Ifnar1*$^{-/-}$ mice infection. In our experimental system (*PbA*-GFP), type I IFN appears to be dominant during other stages of ECM pathogenesis. Despite rapid and steep development of parasitemia throughout infection and parasite accumulation within the brain tissue at levels comparable to susceptible C57BL/6 mice, this was not enough to provoke a sufficient inflammatory response for BBB compromise and mononuclear cell accumulation within brain microvessels. It is worth mentioning that recombinant human IFN-α evoked a striking reduction in parasite burden and protection from ECM in C57BL/6 mice, suggesting that the type I IFN/IFNAR1 system has a role in parasite development (37).

Our data also point to type I IFN/IFNAR1 controlling disease tolerance to malaria. Tolerance is a defense mechanism that does not limit pathogen load (38), and this is in agreement with recent studies that illustrate *Ifnar1*$^{-/-}$ mice providing a survival advantage against *Plasmodium* infection (39). As a side note, the type I IFN/IFNAR1–signaling system can also be regulated by heme oxygenase-1, a stress-response enzyme associated with CM pathogenesis in children, as we reported previously (25).

The development of a novel transfer protocol allowed us to focus on cellular mechanisms involved in ECM protection conferred by IFNAR1. These experiments uncovered that IFNAR1 is needed unequivocally in primed splenic CD8$^+$ T cells to abrogate ECM resistance in *Ifnar1*$^{-/-}$ mice. The cytotoxic profile of CD8$^+$ T cells in ECM induction has been shown using cell transfers; perforin (40) and GrB (41) were identified as essential elements to produce cytotoxicity and effector CD8$^+$ T cell responses. Because we saw no hindrance in the cytotoxic profile of splenic *Ifnar1*$^{-/-}$ CD8$^+$ T cells upon infection (Fig. 7A–C), this suggests that priming in the spleen is not impaired. However, because we observed lower retention of activated CD8$^+$ T cells in the brain of *Ifnar1*$^{-/-}$ ECM-resistant mice, type I IFN could influence ECM via its action in the brain. Type I IFN was shown to be critical in maintaining CD8$^+$ T cells at the site of their effector function (42); therefore, this hints that unresponsive *Ifnar1*$^{-/-}$ CD8$^+$ T cells may have an impaired ability to accumulate within the brain tissue. We question whether enabling the accumulation of IFNAR1$^-$ CD8$^+$ T cells in the brain could generate enough power to trigger an ECM response. We noted that *Ifnar1*$^{-/-}$ mice that received primed CD8$^+$ splenocytes accumulated relatively low numbers of activated CD8$^+$ T cells within the brain tissue, yet they developed ECM (Fig. 7G–I). This supports the hypothesis that induction of ECM in transferred mice was not due to CD8$^+$ T cell accumulation but rather was caused by their expression of IFNAR1, allowing CD8$^+$ T cells to become reactivated by type I IFN within the brain and unleashing their cytotoxic effector capacity.

Evidence also showed that CD8$^+$ T cells require constant Ag presentation to remain at their effector site (43–45). Type I IFN was shown to directly stimulate CD8$^+$ T cell responses during Ag cross-presentation (46). This suggests that resistance of *Ifnar1*$^{-/-}$ CD8$^+$ T cells to inducing ECM could be due to their inability to respond to type I IFN signals during Ag presentation within the brain tissue. Moreover, the exact way in which CD8$^+$ T cells are presented in the brain is still unknown. We hypothesize that IFNAR1 affects CD8$^+$ T cell stimulation at different stages of *Plasmodium* infection. We support the spleen as a primary site of parasite Ag presentation and propose that a secondary site of stimulation and presentation to CD8$^+$ T cells occurs within the brain tissue. In fact, transfer of *Ifnar1*$^{-/-}$ CD8$^-$ splenocytes caused a slight increase in susceptibility to ECM, possibly reflecting the effect of other immune cells, predominantly activated CD4$^+$ T cells, in promoting ECM development (47) by an IFNAR1-independent mechanism.

Ifnar1$^{-/-}$ mice also have proved fundamental in uncovering the therapeutic use of type I IFN in cancer (48), as well as in cases of experimental autoimmune encephalomyelitis (17). However, in support of our results, Ref. 45 reviews how type I IFN therapy has led to the induction of autoimmune diseases. Our results induce us to think that blocking IFNAR1 would be therapeutic for CM protection; however, this would have to done with extreme precision because of the vast array of cells expressing IFNAR1, and, more importantly, this would not directly mimic an *IFNAR1* gene polymorphism.

Our work collectively highlights the cohesive role of *IFNAR1* during CM development, which is that it confers human CM protection and it is implicated in CD8$^+$ T cell pathology in mouse ECM. These observations allow us to speculate that *IFNAR1* may operate in human CM through the stimulation of CD8$^+$ T cells. Together, these results identify responses of type I IFN through IFNAR1 as vital components in CM pathogenesis.

Acknowledgments

We thank Miguel Soares (Instituto Gulbenkian de Ciência) for critical revision of the manuscript and use of reagents and Ivo Marguti for technical support and discussion. We thank Dr. Tânia Carvalho, resident pathologist at Instituto Gulbenkian de Ciência, for analysis of pathology samples and the Cell Imaging Unit for expertise in cell sorting. We are most grateful to the children who participated in the study and thank the staff of the Hospital Pediátrico David Bernardino. We are grateful to Drs. Filomena Silva, Emingarda Castelo Branco, and Rosa Silva from the Instituto de Saúde Pública de Angola in Luanda for help with sample processing and Dr. Rui Pinto (Clínica Sagrada Esperança, Luanda, Angola) for sample collection materials.

Disclosures

The authors have no financial conflicts of interest.

References

1. Issifou, S., E. Kendjo, M. A. Missinou, P. B. Matsiegui, A. Dzeing-Ella, F. A. Dissanami, M. Kombila, S. Krishna, and P. G. Kremsner. 2007. Differences in presentation of severe malaria in urban and rural Gabon. *Am. J. Trop. Med. Hyg.* 77: 1015–1019.
2. Mackintosh, C. L., J. G. Beeson, and K. Marsh. 2004. Clinical features and pathogenesis of severe malaria. *Trends Parasitol.* 20: 597–603.
3. Newton, C. R., and S. Krishna. 1998. Severe falciparum malaria in children: current understanding of pathophysiology and supportive treatment. *Pharmacol. Ther.* 79: 1–53.
4. Milner, D. A., Jr. 2010. Rethinking cerebral malaria pathology. *Curr. Opin. Infect. Dis.* 23: 456–463.
5. Carvalho, L. J. 2010. Murine cerebral malaria: how far from human cerebral malaria? *Trends Parasitol.* 26: 271–272.
6. Craig, A. G., G. E. Grau, C. Janse, J. W. Kazura, D. Milner, J. W. Barnwell, G. Turner, and J. Langhorne; participants of the Hinxton Retreat meeting on Animal Models for Research on Severe Malaria. 2012. The role of animal models for research on severe malaria. *PLoS Pathog.* 8: e1002401.
7. de Souza, J. B., J. C. Hafalla, E. M. Riley, and K. N. Couper. 2010. Cerebral malaria: why experimental murine models are required to understand the pathogenesis of disease. *Parasitology* 137: 755–772.
8. Rénia, L., A. C. Grüner, and G. Snounou. 2010. Cerebral malaria: in praise of epistemes. *Trends Parasitol.* 26: 275–277.
9. Riley, E. M., K. N. Couper, H. Helmby, J. C. Hafalla, J. B. de Souza, J. Langhorne, W. B. Jarra, and F. Zavala. 2010. Neuropathogenesis of human and murine malaria. *Trends Parasitol.* 26: 277–278.
10. Belnoue, E., M. Kayibanda, A. M. Vigario, J. C. Deschemin, N. van Rooijen, M. Viguier, G. Snounou, and L. Rénia. 2002. On the pathogenic role of brain-sequestered alphabeta CD8+ T cells in experimental cerebral malaria. *J. Immunol.* 169: 6369–6375.
11. Hermsen, C., T. van de Wiel, E. Mommers, R. Sauerwein, and W. Eling. 1997. Depletion of CD4+ or CD8+ T-cells prevents *Plasmodium berghei* induced cerebral malaria in end-stage disease. *Parasitology* 114: 7–12.

12. Driss, A., J. M. Hibbert, N. O. Wilson, S. A. Iqbal, T. V. Adamkiewicz, and J. K. Stiles. 2011. Genetic polymorphisms linked to susceptibility to malaria. *Malar. J.* 10: 271.
13. Aucan, C., A. J. Walley, B. J. Hennig, J. Fitness, A. Frodsham, L. Zhang, D. Kwiatkowski, and A. V. Hill. 2003. Interferon-alpha receptor-1 (IFNAR1) variants are associated with protection against cerebral malaria in the Gambia. *Genes Immun.* 4: 275–282.
14. Khor, C. C., F. O. Vannberg, S. J. Chapman, A. Walley, C. Aucan, H. Loke, N. J. White, T. Peto, L. K. Khor, D. Kwiatkowski, et al. 2007. Positive replication and linkage disequilibrium mapping of the chromosome 21q22.1 malaria susceptibility locus. *Genes Immun.* 8: 570–576.
15. Diop, G., T. Hirtzig, H. Do, C. Coulonges, A. Vasilescu, T. Labib, J. L. Spadoni, A. Therwath, M. Lathrop, F. Matsuda, and J. F. Zagury. 2006. Exhaustive genotyping of the interferon alpha receptor 1 (IFNAR1) gene and association of an IFNAR1 protein variant with AIDS progression or susceptibility to HIV-1 infection in a French AIDS cohort. *Biomed. Pharmacother.* 60: 569–577.
16. Ito, T., H. Kanzler, O. Duramad, W. Cao, and Y. J. Liu. 2006. Specialization, kinetics, and repertoire of type 1 interferon responses by human plasmacytoid predendritic cells. *Blood* 107: 2423–2431.
17. Prinz, M., H. Schmidt, A. Mildner, K. P. Knobeloch, U. K. Hanisch, J. Raasch, D. Merkler, C. Detje, I. Gutcher, J. Mages, et al. 2008. Distinct and nonredundant in vivo functions of IFNAR on myeloid cells limit autoimmunity in the central nervous system. *Immunity* 28: 675–686.
18. deWalick, S., F. H. Amante, K. A. McSweeney, L. M. Randall, A. C. Stanley, A. Haque, R. D. Kuns, K. P. MacDonald, G. R. Hill, and C. R. Engwerda. 2007. Cutting edge: conventional dendritic cells are the critical APC required for the induction of experimental cerebral malaria. *J. Immunol.* 178: 6033–6037.
19. Lundie, R. J., T. F. de Koning-Ward, G. M. Davey, C. Q. Nie, D. S. Hansen, L. S. Lau, J. D. Mintern, G. T. Belz, L. Schofield, F. R. Carbone, et al. 2008. Blood-stage *Plasmodium* infection induces CD8+ T lymphocytes to parasite-expressed antigens, largely regulated by CD8alpha+ dendritic cells. *Proc. Natl. Acad. Sci. USA* 105: 14509–14514.
20. O'Connell, R. M., S. K. Saha, S. A. Vaidya, K. W. Bruhn, G. A. Miranda, B. Zarnegar, A. K. Perry, B. O. Nguyen, T. F. Lane, T. Taniguchi, et al. 2004. Type I interferon production enhances susceptibility to *Listeria monocytogenes* infection. *J. Exp. Med.* 200: 437–445.
21. Stockinger, S., and T. Decker. 2008. Novel functions of type I interferons revealed by infection studies with *Listeria monocytogenes. Immunobiology* 213: 889–897.
22. Sharma, S., R. B. DeOliveira, P. Kalantari, P. Parroche, N. Goutagny, Z. Jiang, J. Chan, D. C. Bartholomeu, F. Lauw, J. P. Hall, et al. 2011. Innate immune recognition of an AT-rich stem-loop DNA motif in the *Plasmodium falciparum* genome. *Immunity* 35: 194–207.
23. Haque, A., S. E. Best, A. Ammerdorffer, L. Desbarrieres, M. M. de Oca, F. H. Amante, F. de Labastida Rivera, P. Hertzog, G. M. Boyle, G. R. Hill, and C. R. Engwerda. 2011. Type I interferons suppress $CD4^+$ T-cell-dependent parasite control during blood-stage *Plasmodium* infection. *Eur. J. Immunol.* 41: 2688–2698.
24. e Pinto, E. A., and J. G. Alves. 2008. The causes of death of hospitalized children in Angola. *Trop. Doct.* 38: 66–67.
25. Sambo, M. R., M. J. Trovoada, C. Benchimol, V. Quinhentos, L. Gonçalves, R. Velosa, M. I. Marques, N. Sepúlveda, T. G. Clark, S. Mustafa, et al. 2010. Transforming growth factor beta 2 and heme oxygenase 1 genes are risk factors for the cerebral malaria syndrome in Angolan children. *PLoS ONE* 5: e11141.
26. Greenwood, B. M., and J. R. Armstrong. 1991. Comparison of two simple methods for determining malaria parasite density. *Trans. R. Soc. Trop. Med. Hyg.* 85: 186–188.
27. Barrett, J. C., B. Fry, J. Maller, and M. J. Daly. 2005. Haploview: analysis and visualization of LD and haplotype maps. *Bioinformatics* 21: 263–265.
28. Luna, A., and K. K. Nicodemus. 2007. snp.plotter: an R-based SNP/haplotype association and linkage disequilibrium plotting package. *Bioinformatics* 23: 774–776.
29. González, J. R., L. Armengol, X. Solé, E. Guinó, J. M. Mercader, X. Estivill, and V. Moreno. 2007. SNPassoc: an R package to perform whole genome association studies. *Bioinformatics* 23: 644–645.
30. Müller, U., U. Steinhoff, L. F. Reis, S. Hemmi, J. Pavlovic, R. M. Zinkernagel, and M. Aguet. 1994. Functional role of type I and type II interferons in antiviral defense. *Science* 264: 1918–1921.
31. Franke-Fayard, B., H. Trueman, J. Ramesar, J. Mendoza, M. van der Keur, R. van der Linden, R. E. Sinden, A. P. Waters, and C. J. Janse. 2004. A *Plasmodium berghei* reference line that constitutively expresses GFP at a high level throughout the complete life cycle. *Mol. Biochem. Parasitol.* 137: 23–33.
32. Pamplona, A., A. Ferreira, J. Balla, V. Jeney, G. Balla, S. Epiphanio, A. Chora, C. D. Rodrigues, I. P. Gregoire, M. Cunha-Rodrigues, et al. 2007. Heme oxygenase-1 and carbon monoxide suppress the pathogenesis of experimental cerebral malaria. *Nat. Med.* 13: 703–710.
33. Epiphanio, S., S. A. Mikolajczak, L. A. Gonçalves, A. Pamplona, S. Portugal, S. Albuquerque, M. Goldberg, S. Rebelo, D. G. Anderson, A. Akinc, et al. 2008. Heme oxygenase-1 is an anti-inflammatory host factor that promotes murine plasmodium liver infection. *Cell Host Microbe* 3: 331–338.
34. Ferreira, A., I. Marguti, I. Bechmann, V. Jeney, A. Chora, N. R. Palha, S. Rebelo, A. Henri, Y. Beuzard, and M. P. Soares. 2011. Sickle hemoglobin confers tolerance to *Plasmodium* infection. *Cell* 145: 398–409.
35. Zhou, J., J. D. Huang, V. K. Poon, D. Q. Chen, C. C. Chan, F. Ng, X. Y. Guan, R. M. Watt, L. Lu, K. Y. Yuen, and B. J. Zheng. 2009. Functional dissection of an IFN-alpha/beta receptor 1 promoter variant that confers higher risk to chronic hepatitis B virus infection. *J. Hepatol.* 51: 322–332.
36. Song, H., N. T. Xuan, N. L. Toan, V. Q. Binh, A. B. Boldt, P. G. Kremsner, and J. F. Kun. 2008. Association of two variants of the interferon-alpha receptor-1 gene with the presentation of hepatitis B virus infection. *Eur. Cytokine Netw.* 19: 204–210.
37. Vigário, A. M., E. Belnoue, A. C. Grüner, M. Mauduit, M. Kayibanda, J. C. Deschemin, M. Marussig, G. Snounou, D. Mazier, I. Gresser, and L. Rénia. 2007. Recombinant human IFN-alpha inhibits cerebral malaria and reduces parasite burden in mice. *J. Immunol.* 178: 6416–6425.
38. Medzhitov, R., D. S. Schneider, and M. P. Soares. 2012. Disease tolerance as a defense strategy. *Science* 335: 936–941.
39. Erdman, L. K., and K. C. Kain. 2011. Taking the sting out of malaria. *Immunity* 35: 149–151.
40. Nitcheu, J., O. Bonduelle, C. Combadiere, M. Tefit, D. Seilhean, D. Mazier, and B. Combadiere. 2003. Perforin-dependent brain-infiltrating cytotoxic CD8+ T lymphocytes mediate experimental cerebral malaria pathogenesis. *J. Immunol.* 170: 2221–2228.
41. Haque, A., S. E. Best, K. Unosson, F. H. Amante, F. de Labastida, N. M. Anstey, G. Karupiah, M. J. Smyth, W. R. Heath, and C. R. Engwerda. 2011. Granzyme B expression by CD8+ T cells is required for the development of experimental cerebral malaria. *J. Immunol.* 186: 6148–6156.
42. Marrack, P., J. Kappler, and T. Mitchell. 1999. Type I interferons keep activated T cells alive. *J. Exp. Med.* 189: 521–530.
43. Galea, I., M. Bernardes-Silva, P. A. Forse, N. van Rooijen, R. S. Liblau, and V. H. Perry. 2007. An antigen-specific pathway for CD8 T cells across the blood-brain barrier. *J. Exp. Med.* 204: 2023–2030.
44. Miu, J., N. H. Hunt, and H. J. Ball. 2008. Predominance of interferon-related responses in the brain during murine malaria, as identified by microarray analysis. *Infect. Immun.* 76: 1812–1824.
45. Stewart, T. A. 2003. Neutralizing interferon alpha as a therapeutic approach to autoimmune diseases. *Cytokine Growth Factor Rev.* 14: 139–154.
46. Le Bon, A., V. Durand, E. Kamphuis, C. Thompson, S. Bulfone-Paus, C. Rossmann, U. Kalinke, and D. F. Tough. 2006. Direct stimulation of T cells by type I IFN enhances the CD8+ T cell response during cross-priming. *J. Immunol.* 176: 4682–4689.
47. Villegas-Mendez, A., R. Greig, T. N. Shaw, J. B. de Souza, E. Gwyer Findlay, J. S. Stumhofer, J. C. Hafalla, D. G. Blount, C. A. Hunter, E. M. Riley, and K. N. Couper. 2012. IFN-γ-producing CD4+ T cells promote experimental cerebral malaria by modulating CD8+ T cell accumulation within the brain. *J. Immunol.* 189: 968–979.
48. Johns, T. G., I. R. Mackay, K. A. Callister, P. J. Hertzog, R. J. Devenish, and A. W. Linnane. 1992. Antiproliferative potencies of interferons on melanoma cell lines and xenografts: higher efficacy of interferon beta. *J. Natl. Cancer Inst.* 84: 1185–1190.

Supplemental Figures

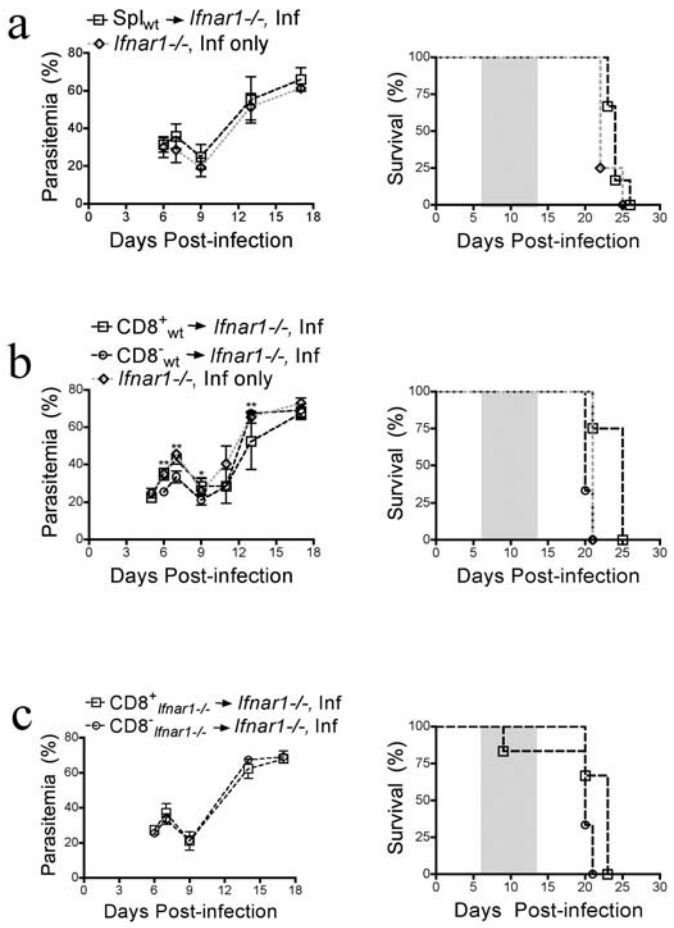

Figure S1. Transfer of non-exposed CD8$^+$ C57BL/6 cells cannot induce ECM in *Ifnar1*$^{-/-}$ mice. (a) *Ifnar1*$^{-/-}$ mice that received total spleen cells (open squares) from C57BL/6 non-exposed mice; transfer control is represented by infected *Ifnar1*$^{-/-}$ mice that received no cell transfer (diamonds). (b) *Ifnar1*$^{-/-}$ recipient mice that received sorted CD8$^+$ spleen cells (open squares) or sorted CD8-depleted spleen cells (open circles) from C57BL/6 non-exposed mice; transfer control is represented by infected *Ifnar1*$^{-/-}$ mice that received no cell transfer (diamonds). (c) *Ifnar1*$^{-/-}$ mice that received sorted CD8$^+$ spleen cells (open squares) or sorted CD8$^-$ depleted spleen cells (open circles) from *Ifnar1*$^{-/-}$ mice. (n = 3-6 mice per group, parasitemia; unpaired, two tailed t-test performed between CD8$^+$ and CD8-depleted cell transfer recipient groups; *$P \leq 0.05$, **$P \leq 0.01$, survival curves; Log-rank Test). Each plot represents one of at least two independent experiments performed. Time window of C57BL/6 ECM manifestations is shadowed in survival plots.

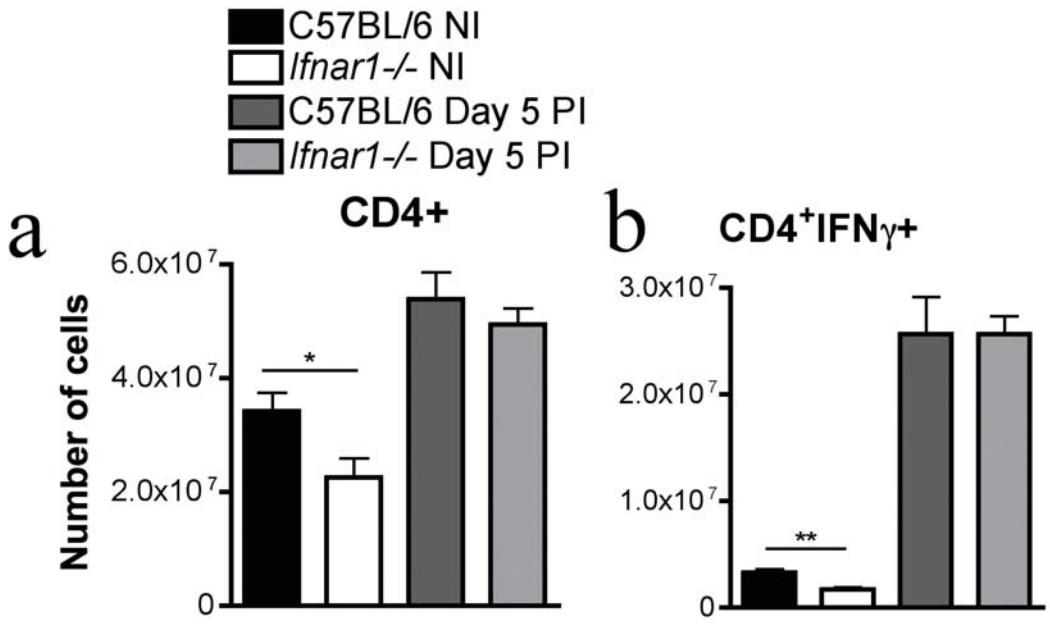

Figure S2. *Ifnar1*$^{-/-}$ mice show no significant difference in CD4^{+} T cell numbers and activation profile compared to C57BL/6 mice upon infection. Total number of CD4^{+} T cells (a) and IFN-γ+ CD4^{+} T cells (b) in the spleen of non-infected (NI) and infected C57BL/6 and *Ifnar1*$^{-/-}$ mice. Mice were infected 1×10^{6} *PbA*, analyzed on day 5 PI. (n = 3-5 mice per group, non-parametric two tailed Mann Whitney test; *$P \leq 0.05$, **$P \leq 0.01$). Data is representative of two independent experiments performed.

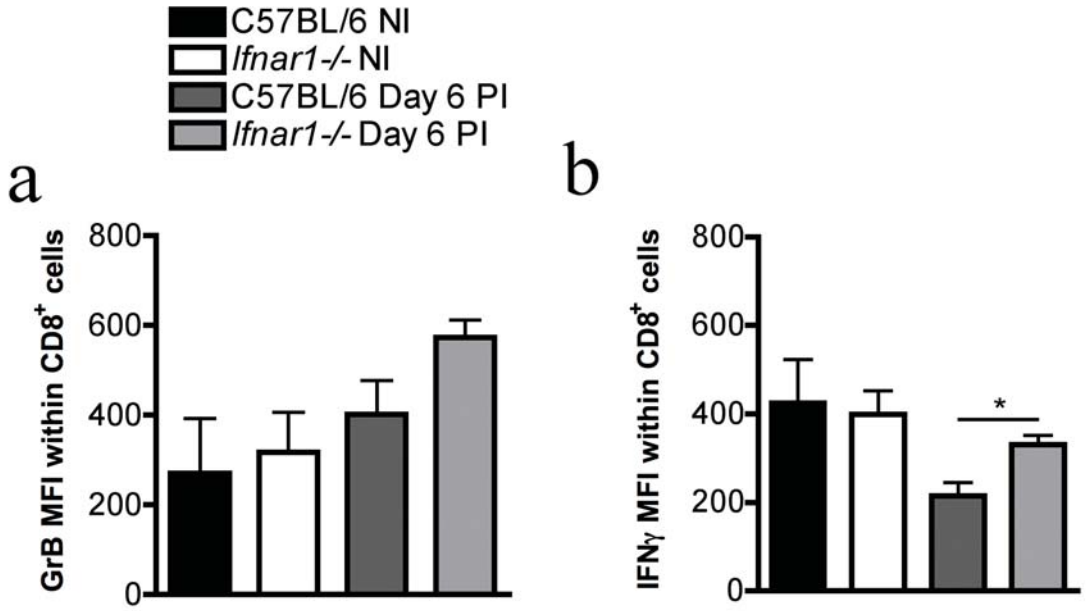

Figure S3. *Ifnar1*$^{-/-}$ CD8^{+} T cells show cytotoxic ability like that of C57BL/6 mice. Mean fluorescence intensity (MFI) of GrB+ on CD8^{+} T cells (a) and IFN-γ+ on CD8^{+} T cells (b) in perfused brains of infected and non-infected C57BL/6 and *Ifnar1*$^{-/-}$ mice, infected 1×10^{6} *PbA*, on day 6 PI when C57BL/6 displayed symptoms of ECM development. (n = 3-5 mice per group, unpaired, two tailed t-test; *$P \leq 0.05$. Data is representative of three independent experiments performed

Supplemental Table 1. Results of SNP genotypic association in *IFNAR1* gene at 21q22.1 with progression to cerebral malaria (CM vs UM).

						Genotype numbers (frequency %)		CM vs UM		
SNP ID	SNP reference	Position (Mb)	Alleles[a]	Gene region	Genotypes	CM (n=110)	UM (n=129)	P-value$_{adj}$	OR(95% CI)	P-value$_{corr}$
1	rs2834190	34693011	A/T	Promoter	A/A	99 (90.8)	113 (87.6)	0.39981		NS
					T/A-T/T	10 (9.2)	16 (12.4)			
2	rs9984439	34693063	A/G	Promoter	A/A	60 (55.0)	48 (38.1)	**1.05E-02**	0.51 (0.30-0.86)	NS
					A/G-G/G	49 (45.0)	78 (61.9)			
3	rs2843710	34696707	C/G	Promoter	C/C	63 (57.3)	49 (38.0)	**2.95E-03**	0.46 (0.27-0.77)	NS
					C/G-G/G	47 (42.7)	80 (62.0)			
4	rs2856968	34697981	A/G	Intron 1	A/A	70 (70.7)	49 (38.6)	**1.33E-06**	0.26 (0.15-0.46)	**2.39E-05**
					G/A-G/G	29 (29.3)	78 (61.4)			
5	rs2856969	34698159	A/G	Intron 1	A/A	60 (55.6)	49 (38.0)	**7.68E-03**	0.49 (0.29-0.83)	NS
					A/G-G/G	48 (44.4)	80 (62.0)			
6	rs2243590	34704276	C/T	Intron 1	C/C	60 (56.1)	49 (39.2)	**1.09E-02**	0.51 (0.30-0.86)	NS
					C/T-T/T	47 (43.9)	76 (60.8)			
7	rs2252931	34704320	A/G	Intron 1	G/G	99 (90.0)	113 (87.6)	0.53163		NS
					A/G-A/A	11 (10.0)	16 (12.4)			
8	rs2834193	34704660	C/T	Intron 1	C/C	100 (92.6)	116 (89.9)	0.49431		NS
					C/T-T/T	8 (7.4)	13 (10.1)			
9	rs2253923	34712419	A/T	Intron 2	A/A	68 (63.6)	48 (37.2)	**5.77E-05**	0.34 (0.20-0.58)	**1.04E-03**
					T/A-T/T	39 (36.4)	81 (62.8)			
10	rs9981753	34713317	C/T	Exon 3	T/T	101 (93.5)	114 (89.1)	NA	NA	NA
					T/C-C/C	NA	14 (10.9)			
11	rs2257167	34715699	C/G	Exon 4	G/G	83 (75.5)	80 (63.0)	**4.25E-02**	0.56 (0.32-0.99)	NS
					G/C-C/C	27 (24.5)	47 (37.0)			
12	rs17875834	34721782	C/T	Exon 8	C/C	69 (62.7)	87 (67.4)	0.41577		NS
					T/C-T/T	41 (37.3)	42 (32.6)			
13	rs2254180	34726230	C/T	Intron 10	T/T	74 (77.9)	82 (64.1)	**2.76E-02**	0.51 (0.28-0.94)	NS
					C/T-C/C	21 (22.1)	46 (35.9)			
14	rs7279125	34727015	A/C	Intron 10	A/A	101 (91.8)	116 (89.9)	0.56636		NS
					C/A-C/C	9 (8.2)	13 (10.1)			
15	rs2834199	34727516	A/G	Intron 10	G/G	99 (91.7)	116 (89.9)	0.66515		NS
					A/G-A/A	9 (8.3)	13 (10.1)			
16	rs2834202	34730954	A/G	Exon 11	A/A	90 (81.8)	91 (70.5)	**4.58E-02**	0.54 (0.29-1.00)	NS
					G/A-G/G	20 (18.2)	38 (29.5)			
17	rs8130745	34733770	C/T	Downstream	T/T	102 (92.7)	123 (95.3)	0.32947		NS
					C/T-C/C	8 (7.3)	6 (4.7)			
18	rs9980664	34734510	A/C	Downstream	C/C	64 (64.0)	64 (50.0)	**3.32E-02**	0.56 (0.33-0.96)	NS
					C/A-A/A	36 (36.0)	64 (50.0)			

The genetic association P-values are under the dominant model and adjusted for age. Numbers of genotypes are given along with percentages within each group (CM, UM) within parentheses. Univariately significant P-values (P-value$_{adj}$; <0.05) and significant Bonferroni corrected P-values (P-value$_{corr}$; <0.05) are highlighted in bold. Abbreviations: CM, cerebral malaria; UM, uncomplicated malaria; Mb, Megabases; OR, odds ratio; 95% CI, 95% confidence interval; NA, not available; NS, not significant; a, Major/minor allele.